

Dichloro(4,10-dimethyl-1,4,7,10-tetraazabicyclo[5.5.2]tetradecane)-iron(III) hexafluorophosphate

James M. McClain II,^a Danny L. Maples,^a Randall D. Maples,^a Dallas L. Matz,^a Sebastian M. Harris,^a Andrew D. L. Nelson,^a Jon D. Silversides,^b Stephen J. Archibald^{b*} and Timothy J. Hubin^{a*}

^aDepartment of Chemistry and Physics, Southwestern Oklahoma State University, Weatherford, OK 73096, USA, and ^bDepartment of Chemistry, University of Hull, Cottingham Road, Hull HU6 7RX, England

Correspondence e-mail: s.j.archibald@hull.ac.uk, tim.hubin@sosu.edu

Received 8 September 2006

Accepted 3 October 2006

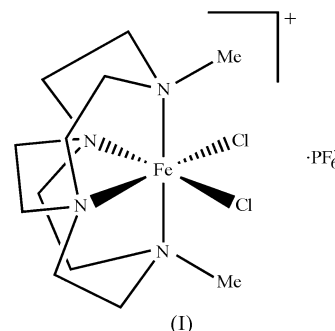
Online 31 October 2006

The title compound, $[\text{FeCl}_2(\text{C}_{12}\text{H}_{26}\text{N}_4)]\text{PF}_6$, is the first mononuclear Fe^{3+} complex of an ethylene cross-bridged tetraaza-macrocyclic to be structurally characterized. Comparison with the mononuclear Fe^{2+} complex of the same ligand shows that the smaller Fe^{3+} ion is more fully encapsulated by the cavity of the bicyclic ligand. Comparison with the μ -oxo dinuclear complex of an unsubstituted ligand of the same size demonstrates that the methyl groups of 4,10-dimethyl-1,4,7,10-tetraazabicyclo[5.5.2]tetradecane prevent dimerization upon oxidation of the metal centre. $\text{N}_{\text{ax}}-\text{Fe}^{3+}-\text{N}_{\text{ax}}$ bond angles (ax is axial), and thus the degree of encapsulation by the ligand, are quite different between the mononuclear and dinuclear μ -oxo species, which is probably the consequence of steric considerations.

Comment

The tendency for iron complexes to form rust limits the utility, especially in aqueous media, of functional catalysts based on common ligands (Ortiz de Montellano, 1986). Even so, iron is one of the predominant metal ions found in biological catalytic systems (Jang *et al.*, 1991; Wallar & Lipscomb, 1996; Boyington *et al.*, 1993). A major feature of numerous synthetic catalysts having familiar nitrogen donors and vacant coordination sites is their propensity to form dimers in which higher-valent metal ions are present. One of us has produced iron(II) (Hubin *et al.*, 2000) and iron(III) (Hubin *et al.*, 2001) complexes of ethylene cross-bridged tetraaza-macrocyclic ligands that are remarkably resistant to oxidative hydrolysis while still having available sites for binding of the metal ion to either a terminal oxidant or a substrate. The ability of the complex to remain mononuclear, and thus catalytically useful, appears to hinge on the substitution pattern of the non-bridgehead N atoms of the bicyclic ligands (Hubin *et al.*, 2001).

Methyl or benzyl substitution results only in mononuclear complexes, even in the M^{3+} (Hubin *et al.*, 2001, 2003) or M^{4+} (Yin *et al.*, 2006) oxidation state, while oxidation of the unsubstituted ligand complexes results in μ -oxo iron(III) dimers (Hubin *et al.*, 2003).



Structural characterization of an Fe^{3+} mononuclear complex has not been achieved prior to the present study, which (i) demonstrates that even upon oxidation the methyl-substituted ligand does not allow dimerization to occur and (ii) provides a structure for comparison to the lower valent analogue and to the unsubstituted analogue's iron(III) μ -oxo dimer. Comparison of the Fe^{3+} 4,10-dimethyl-1,4,7,10-tetraazabicyclo[5.5.2]tetradecane dichloride complex, (I) (Fig. 1 and Table 1), with the Fe^{2+} 4,10-dimethyl-1,4,7,10-tetraazabicyclo[5.5.2]tetradecane dichloride complex primarily demonstrates the reduction in ionic radius of the iron ion upon oxidation. The $\text{N}_{\text{ax}}-\text{Fe}^{3+}-\text{N}_{\text{ax}}$ angle (ax is axial) is $153.20(9)^\circ$ in (I), while the $\text{N}_{\text{ax}}-\text{Fe}^{2+}-\text{N}_{\text{ax}}$ angle is $146.91(7)^\circ$ in the reduced complex (Hubin *et al.*, 2000). The smaller Fe^{3+} ion is pulled further into the ligand cavity as the favored octahedral geometry is approached. Interestingly, the two methyl substituents are almost exactly eclipsed when viewed down the $\text{N}_{\text{ax}}-\text{Fe}^{2+}-\text{N}_{\text{ax}}$ axis, as might be expected from the symmetry of the complex (Fig. 2). However, they are more skewed in the

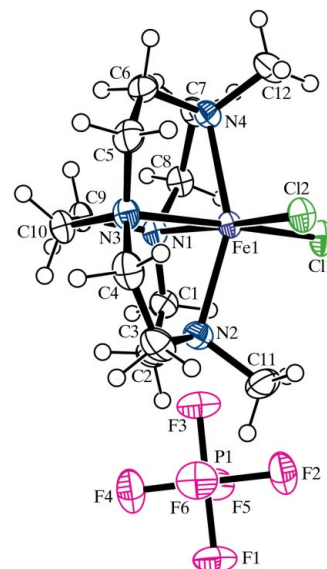


Figure 1
The structure of (I), with displacement ellipsoids drawn at the 50% probability level.

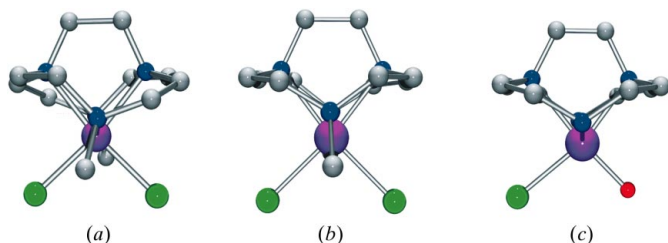


Figure 2
Comparison of the Fe^{3+} monomeric complex (a) from this work with (b) the equivalent Fe^{2+} complex and (c) the Fe^{3+} dimer formed with the unsubstituted ligand. All views are oriented to look down the $\text{N}_{\text{ax}}-\text{Fe}-\text{N}_{\text{ax}}$ axis. The methyl groups in the Fe^{3+} complex are skewed, whereas they are eclipsed in the Fe^{2+} complex. For the sake of clarity, H atoms have been omitted.

Fe^{3+} structure. Perhaps the ligand must twist to accommodate the Fe^{3+} ion further into the ligand cavity. The $\text{Fe}-\text{N}$ bond lengths are also affected, having an average of 2.26 Å in the Fe^{2+} complex and 2.17 Å in the Fe^{3+} complex.

Comparison of the Fe^{3+} monomer with the μ -oxo dimer complex is also informative. The secondary amine- Fe^{3+} bond lengths in the dimer are similar to the tertiary amine- Fe^{3+} bond lengths; the $\text{Fe}-\text{N}$ (secondary) distances average 2.17 Å, with one longer $\text{Fe}-\text{N}$ (tertiary) bond of 2.258 (5) Å (see Table 2). This may be associated with the asymmetric accommodation of a longer $\text{Fe}-\text{Cl}$ bond and a shorter $\text{Fe}-\text{O}$ bond. In the monomer, with all tertiary amines, the average $\text{Fe}-\text{N}$ bond distance is 2.17 Å, matching the shorter $\text{Fe}-\text{N}$ bonds in the dimer. The $\text{N}_{\text{ax}}-\text{Fe}-\text{N}_{\text{ax}}$ bond angle averages 147.6 (2)° in the dimer, while this value is 153.20 (9)° in the monomer. Clearly, dimerization and its associated steric consequences push the Fe^{3+} ion further out of the ligand cavity than it is in the Fe^{3+} monomer. In fact, the dimer $\text{N}_{\text{ax}}-\text{Fe}-\text{N}_{\text{ax}}$ bond angle is much closer to that of the Fe^{2+} monomer [146.91 (7)°] than that of the Fe^{3+} monomer [153.20 (9)°; Table 2]. This steric consequence is consistent with the observation that the more sterically demanding methyl-substituted ligand prevents dimerization altogether. This is supported by a comparison of all three structures viewed along the $\text{N}_{\text{ax}}-\text{Fe}-\text{N}_{\text{ax}}$ axis, where a skewing of the methyl groups and a twist in the macrocyclic backbone are observed for the Fe^{3+} monomer relative to the other two structures (Fig. 2).

Experimental

The title complex was prepared by a procedure slightly modified from those described by Hubin *et al.* (2000, 2001). In an inert atmosphere glove-box, 4,10-dimethyl-1,4,7,10-tetraazabicyclo[5.5.2]tetradecane (0.226 g, 0.001 mol) [prepared according to the procedure described by Wong *et al.* (2000)] was dissolved in acetonitrile (20 ml) in a 50 ml Erlenmeyer flask. Anhydrous iron(II) chloride (0.127 g, 0.001 mol) was added to the stirring ligand solution. The reaction was stirred at room temperature overnight. Dimethylformamide (12 ml) was added to dissolve a purple solid that had formed, and the reaction was then stirred for an additional 3 h, during which time the solid dissolved to give a light-brown solution. The solution was then filtered through filter paper and the solvent was removed under vacuum to give a brown solid, *viz.* the iron(II) dichloride complex of 4,10-dimethyl-1,4,7,10-tetraazabicyclo[5.5.2]tetradecane. In the glove-box, the

divalent iron complex was dissolved in methanol (20 ml) in a round-bottomed flask. Five equivalents of NH_4PF_6 (0.005 mol, 0.815 g) were dissolved in the solution. The flask was stoppered to protect it from air before being removed from the glove-box. In a fume-hood, a stream of nitrogen gas was directed over the surface of the solution. Br_2 (4–6 drops) was added and the reaction was stirred for 15 min. A bright-yellow precipitate formed immediately. The nitrogen gas was allowed to bubble through the solution for 15 min to remove excess Br_2 . The flask was then stoppered and placed in a freezer for 30 min to complete the precipitation. The yellow solid product was collected by vacuum filtration on a glass frit and washed successively with methanol and ether. The product was analytically pure as calculated with one-third molar equivalents of water of crystallization. X-ray quality crystals were grown from ether diffusion into an acetonitrile solution.

Crystal data

$[\text{FeCl}_2(\text{C}_{12}\text{H}_{26}\text{N}_4)]\text{PF}_6$	$Z = 4$
$M_r = 498.09$	$D_x = 1.656 \text{ Mg m}^{-3}$
Monoclinic, $P2_1/c$	Mo $K\alpha$ radiation
$a = 8.3437 (12) \text{ \AA}$	$\mu = 1.16 \text{ mm}^{-1}$
$b = 19.848 (2) \text{ \AA}$	$T = 150 (2) \text{ K}$
$c = 14.028 (2) \text{ \AA}$	Block, orange
$\beta = 120.685 (10)^\circ$	$0.49 \times 0.38 \times 0.26 \text{ mm}$
$V = 1997.8 (5) \text{ \AA}^3$	

Data collection

Stoe IPDS-II image plate diffractometer	5655 independent reflections
ω scans	3799 reflections with $I > 2\sigma(I)$
13147 measured reflections	$R_{\text{int}} = 0.039$
	$\theta_{\text{max}} = 30^\circ$

Refinement

Refinement on F^2	$w = 1/[\sigma^2(F_o^2) + (0.0692P)^2]$
$R[F^2 > 2\sigma(F^2)] = 0.041$	where $P = (F_o^2 + 2F_c^2)/3$
$wR(F^2) = 0.117$	$(\Delta/\sigma)_{\text{max}} = 0.026$
$S = 0.97$	$\Delta\rho_{\text{max}} = 0.75 \text{ e \AA}^{-3}$
5655 reflections	$\Delta\rho_{\text{min}} = -0.73 \text{ e \AA}^{-3}$
236 parameters	Extinction correction: <i>SHELXL97</i>
H-atom parameters constrained	Extinction coefficient: 0.0022 (5)

Table 1

Selected geometric parameters (Å, °).

Fe1—Cl1	2.2853 (8)	Fe1—Cl2	2.2911 (7)
N4—Fe1—N3	81.26 (9)	N1—Fe1—Cl1	92.29 (6)
N2—Fe1—N1	81.74 (8)	N2—Fe1—Cl2	96.51 (6)
N4—Fe1—N1	77.85 (8)	N4—Fe1—Cl2	101.50 (6)
N3—Fe1—N1	78.62 (8)	N3—Fe1—Cl2	93.99 (6)
N2—Fe1—Cl1	100.39 (7)	N1—Fe1—Cl2	172.60 (6)
N4—Fe1—Cl1	97.62 (6)	Cl1—Fe1—Cl2	95.10 (3)
N3—Fe1—Cl1	170.88 (6)		

Table 2

Comparative geometrical parameters (Å, °) for the macrocyclic cavity in Fe^{2+} and Fe^{3+} complexes.

Parameter ^a	$\text{Fe}^{3+}\text{Me}_2\text{L}^b$	$\text{Fe}^{2+}\text{Me}_2\text{L}^c$	$\text{Fe}^{3+}\text{H}_2\text{L}$ dimer ^d
Fe—N1	2.179 (2)	2.240 (2)	2.162 (6)
Fe—N2	2.158 (2)	2.270 (2)	2.169 (5)
Fe—N3	2.171 (2)	2.246 (2)	2.186 (5)
Fe—N4	2.163 (2)	2.263 (2)	2.258 (5)
N2 _{ax} —Fe—N4 _{ax}	153.20 (9)	146.91 (7)	147.6 (2)
N1 _{eq} —Fe—N3 _{eq}	77.81 (9)	77.15 (7)	77.7 (2)

Notes: (a) where there are two independent molecules in the asymmetric unit, an average value is given; (b) this work; (c) Hubin *et al.* (2003); (d) Hubin *et al.* (2000).

H atoms were placed in idealized positions and refined using a riding model, with C–H distances of 0.96 and 0.97 Å for CH₃ and CH₂ H atoms, respectively, and with $U_{\text{iso}}(\text{H})$ values of, respectively, 1.5 and 1.2 times U_{eq} of the carrier atom.

Data collection: *X-AREA* (Stoe & Cie, 2002); cell refinement: *X-AREA*; data reduction: *X-RED* (Stoe & Cie, 2002); program(s) used to solve structure: *SHELXS97* (Sheldrick, 1997); program(s) used to refine structure: *SHELXL97* (Sheldrick, 1997); molecular graphics: *ORTEP* (Johnson, 1965) and *ORTEP-3* (Farrugia, 1997); software used to prepare material for publication: *SHELXL97* and *WinGX* (Farrugia, 1999).

We thank the Chemistry Department of Southwestern Oklahoma State University for its support of this work, which was carried in the Spring 2006 Inorganic Chemistry Lab course CHEM 3234. The X-ray data were collected at the University of Hull using a diffractometer purchased with funds from the EPSRC. We acknowledge the EPSRC's Chemical Database Service at Daresbury, England (Fletcher *et al.*, 1996).

Supplementary data for this paper are available from the IUCr electronic archives (Reference: SK3055). Services for accessing these data are described at the back of the journal.

References

- Boyington, J. C., Gaffney, B. J. & Amzel, L. M. (1993). *Science*, **260**, 1482–1486.
- Farrugia, L. J. (1997). *J. Appl. Cryst.* **30**, 565.
- Farrugia, L. J. (1999). *J. Appl. Cryst.* **32**, 837–838.
- Fletcher, D. A., McMeeking, R. F. & Parkin, D. (1996). *J. Chem. Inf. Comput. Sci.* **36**, 746–749.
- Hubin, T. J., McCormick, J. M., Alcock, N. W. & Busch, D. H. (2001). *Inorg. Chem.* **40**, 435–444.
- Hubin, T. J., McCormick, J. M., Collinson, S. R., Alcock, N. W., Clase, H. J. & Busch, D. H. (2003). *Inorg. Chim. Acta*, **346**, 76–86.
- Hubin, T. J., McCormick, J. M., Collinson, S. R., Buchalova, M., Perkins, C. M., Alcock, N. W., Kahol, P. K., Raghunathan, A. & Busch, D. H. (2000). *J. Am. Chem. Soc.* **122**, 2512–2522.
- Jang, H. G., Cox, D. D. & Que, L. Jr (1991). *J. Am. Chem. Soc.* **113**, 9200–9204.
- Johnson, C. K. (1965). *ORTEP*. Report ORNL-3794. Oak Ridge National Laboratory, Tennessee, USA.
- Ortiz de Montellano, P. R. (1986). In *Cytochrome P450: Structure, Mechanism, and Biochemistry*. New York: Plenum Press.
- Sheldrick, G. M. (1997). *SHELXS97* and *SHELXL97*. University of Göttingen, Germany.
- Stoe & Cie (2002). *X-AREA* and *X-RED*. Stoe & Cie, Darmstadt, Germany.
- Waller, B. J. & Lipscomb, J. D. (1996). *Chem. Rev.* **96**, 2625–2657.
- Wong, E. H., Weisman, G. R., Hill, D. C., Reed, D. P., Rogers, M. E., Condon, J. S., Fagan, M. A., Calabrese, J. C., Lam, K.-C., Guzei, I. A. & Rheingold, A. L. (2000). *J. Am. Chem. Soc.* **122**, 10561–10572.
- Yin, G., Buchalova, M., Danby, A. M., Perkins, C. M., Kitko, D., Carter, J. D., Scheper, W. M. & Busch, D. H. (2006). *Inorg. Chem.* **45**, 3467–3474.